

Spatial and Temporal Distribution Characteristics of Drought in Jilin Province Based on SPEI

Ruixiang Song¹, Tian Li¹, Lifang Song¹, Xinjing Zhang^{2,*}, Xiyu Zhang³, Ying Liu⁴

¹Jilin Meteorological Service Centre, Changchun, Jilin, 130062, China

²Jilin Meteorological Information Network Centre, Changchun, Jilin, 130062, China

³Jilin Shengcai Meteorological Technology Co., Ltd, Changchun, Jilin, 130062, China

⁴Jilin Zhonghe Big Data Technology Co., Ltd, Changchun, Jilin, 130062, China

*Corresponding Author.

Abstract: To investigate the variations in the Jilin Province's drought over time, both in terms of time and space, this study used the monthly precipitation data from 47 stations in Jilin Province for 58 years (1961-2018) and estimated the potential evapotranspiration at each station using the Thorn Thwaite method. The Standardized Precipitation Evapotranspiration Index (SPEI) was calculated for the region, and based on this, the frequency of drought occurrence(FDO) was analyzed for the entire year, each season, and different drought levels. The Mann-Kendall test and Rotation Empirical Orthogonal Function (REOF) analysis were employed to explore the spatial and temporal distribution characteristics of drought in Jilin Province over the past 58 years. The findings indicated that: (1) The Jilin Province experienced an annual drought frequency (DF) ranging from 22% to 40%. The average frequency of the following drought levels was observed: The order of drought intensity is mild, moderate, severe, and extreme. At the seasonal scale, drought occurrence frequencies were relatively high in all four seasons, with higher frequencies in summer, autumn, and winter compared to spring. (2) The annual average SPEI in Jilin Province showed an overall decreasing trend(DT), with a rate of $-0.0072 \cdot a^{-1}$ per year, indicating a tendency towards aridification in the region. The trend in spring SPEI change was the smallest among the four seasons, while autumn showed the highest DT, and winter exhibited the most significant trend towards wetter conditions. (3) The REOF analysis divided Jilin Province into four drought characteristic regions: northwest, central, south, and east.

After 1992, the northwest region experienced a notable shift from wet to dry conditions, with an increasing trend(IT) towards aridification. The central region showed no significant trend in time coefficients, while the time coefficients in the eastern region exhibited intermittent changes. The southern region showed no apparent trend in time coefficients, but the frequency of drought occurrence increased after 1997, indicating a worsening trend of aridification.

Keywords: Jilin Province; SPEI; Temporal and Spatial Distribution of Drought; REOF; Division into Districts

1. Introduction

Drought, being the most common natural disaster globally, often leads to severe environmental issues and significantly impacts agricultural activities, human life, and the development of socio-economic [1,2]. According to statistics, drought-related losses in China account for over 15% of all natural disasters, with the FDO representing one-third of the total frequency of disasters, making it the most prominent among various calamities. China endured protracted, severe droughts that affected the nation's economy and society significantly in the second half of the 20th century[3]. With the gradual warming of the global climate and the rising frequency of severe weather events, drought disaster frequency and intensity have clearly increased over time.

Drought is the primary meteorological disaster in Jilin Province and has a significant impact on the province's economy and food crops. However, there is a lack of extensive research on drought specific to Jilin Province,

particularly regarding the analysis and suitability of drought indices. Many studies on drought indices in this region have only focused on precipitation factors, such as Zhu[4], who used the Z-index as a drought indicator, revealing the drought distribution patterns in the western region of Jilin Province. Yue et al. utilized the Standardized Precipitation Index (SPI) as a drought indicator to analyze the spatiotemporal variation characteristics of drought intensity, extent, and frequency within Jilin Province. These two drought indices, in their computation process, solely consider precipitation, without comprehensive consideration of other influencing factors. Building upon the SPI, Vicente-Serrano et al. proposed the SPEI, which incorporates both precipitation and potential evapotranspiration, thereby providing a more accurate assessment of drought conditions in a particular area[5]. Xu et al. highlighted that SPEI demonstrates better applicability than SPI when evaluating drought and flooding situations in the northeastern region[6]. When calculating the SPEI drought index, two primary methods are commonly employed: the Thornthwaite formula recommended by Vicente-Serrano[7,8] to calculate potential evapotranspiration (PET) and the Food and Agriculture Organization's Penman-Monteith (PM) equation as an alternative for calculating PET instead of the Thornthwaite method. In this study, the Thornthwaite method was mainly utilized to compute PET, which takes into account temperature variations, requires fewer input variables, and provides a straightforward calculation approach that accurately reflects surface potential evapotranspiration.

This study used the Thornthwaite method to calculate potential evapotranspiration and monthly temperature and precipitation data from 47 meteorological stations in Jilin Province from 1961 to 2018. By employing this data, the SPEI was calculated at different temporal scales, including yearly and seasonal scales. Furthermore, the spatiotemporal variation of SPEI in the region was analyzed. The aim of this study is to provide scientific evidence for agricultural production, drought research, and disaster prevention and mitigation in Jilin Province.

2.Data and Methodology

2.1 Overview and Data of the Study Area

In the center of northeastern China, between 122 and 131 degrees east longitude and 41 and 46 degrees north latitude, is the province of Jilin. It spans an area of 187,400 square kilometers, accounting for 2% of the national territory. The climate in this region belongs to a temperate continental monsoon climate, characterized by distinct continental features. With the ongoing climate warming, frequent occurrences of drought disasters have been observed, with wide-ranging implications and significant impact.

The data used in this study were monthly meteorological records from 1961 to 2018, provided by the Jilin Provincial Information Center. The study primarily focused on variables such as precipitation and temperature. To ensure data comprehensiveness, a careful selection was made, incorporating records from a total of 47 meteorological stations. Figure 1 depicts the precise distribution of these stations.

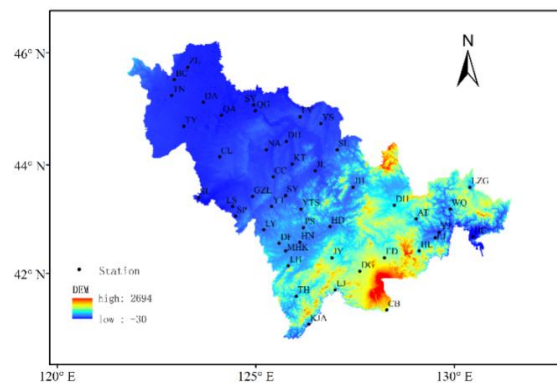


Figure 1. Spatial distribution of 47 meteorological stations in Jilin Province

2.2 Methodology

2.2.1 SPEI

The accumulated probability of the discrepancy between precipitation and potential evapotranspiration (PET) is normalized using a normal distribution to create the SPEI index. SPEI is an optimized version of the SPI calculation method. It utilizes monthly precipitation and mean temperature variables as input to establish cumulative water balance series at diverse time dimensions based on the difference between precipitation and PET. Two methods commonly used to calculate PET are the

Thornthwaite method and the Penman-Monteith equation recommended by the United Nations Food and Agriculture Organization. In this study, the Thornthwaite method was primarily employed to figure PET due to its consideration of temperature variations, simplicity in terms of required input variables, and ability to effectively reflect surface potential evapotranspiration. The specific calculation process is as follows[9]:

$$PET = 16 \times \left(\frac{10T_i}{H}\right)^A \tag{1}$$

$$H = \sum_{i=1}^{12} H_i = \sum_{i=1}^{12} \left(\frac{T_i}{5}\right)^{1.514} \tag{2}$$

Where,

PET =the potential evapotranspiration;

T_i =the monthly average temperature;

H =the heat index of the year;

and A = the constant.

$$A = 0.49 + 0.179H - 0.0000771H^2 + 0.000000675H^3$$

Next, the monthly disparity between evapotranspiration and precipitation was computed. The formula is as follows:

$$D_i = P_i - PET_i \tag{3}$$

Where,

D_i =the difference between precipitation and evapotranspiration;

P_i =the monthly precipitation;

And PET_i =the monthly evapotranspiration.

In the third step, since the original data series may contain negative values, a three-parameter log-logistic probability distribution was used to standardize the precipitation-evapotranspiration difference series. The SPEI for each value was calculated as follows:

$$F(x) = \left[1 + \left(\frac{\alpha}{x - \gamma} \right)^\beta \right]^{-1} \tag{4}$$

Where, the parameters α , β , γ are scale parameter, shape parameter and original parameter respectively, estimated using the method of moments. The calculation is as follows:

$$\alpha = \frac{(\omega_0 - 2\omega_1)\beta}{\Gamma(1+1/\beta)\Gamma(1-1/\beta)} \tag{5}$$

$$\beta = \frac{2\omega_1 - \omega_0}{6\omega_1 - \omega_0 - 6\omega_2} \tag{6}$$

$$\gamma = \omega_0 - \alpha\Gamma(1+1/\beta)\Gamma(1-1/\beta) \tag{7}$$

Where, Γ is the factorial function; ω_0 , ω_1 , and ω_2 are the probability weighted moments of data series D_i :

$$\omega_s = \frac{1}{N} \sum_{i=1}^N (1-F_i)^s D_i \tag{8}$$

$$F_i = \frac{i - 0.35}{N} \tag{9}$$

Where,

N =the number of months.

Finally, the cumulative probability density was standardized and the SPEI was calculated as follows:

$$P = 1 - F(x) \tag{10}$$

$$SPEI = w - \frac{c_0 + c_1w + c_2w^2}{1 - d_1w + d_2w^2 + d_3w^3} \tag{11}$$

$$w = \sqrt{-2\ln(P)} \tag{12}$$

Where, P is the cumulative probability, which satisfies $P \leq 0.5$, similar to the calculation of SPEI.

To capture both the details and overall characteristics of drought processes in the study area, the analysis focused on the seasonal and interannual drought variations at each station. In this study, a 3-month time scale was used to represent seasons, and a 12-month time scale was used to represent interannual variations. There were four seasons: fall, winter, summer, and spring. The drought severity was divided into five levels, as displayed in Table 1:

Table 1. SPEI Drought Severity Levels

Drought degree	SPEI	Drought type
1	SPEI>-0.5	No drought
2	-1.0<SPEI<=-0.5	Mild drought

3	$-1.5 < \text{SPEI} \leq -1.0$	Moderate drought
4	$-2.0 < \text{SPEI} \leq -1.5$	Severe drought
5	$\text{SPEI} \leq -2.0$	Extreme drought

2.2.2 Drought frequency

The FDO at a particular station over the course of the study period is evaluated using DF. The following is the calculating formula:

$$P_i = \frac{n}{N} * 100\% \quad (13)$$

Where,

N = the total number of years with drought occurrence at the station;

n = the total number of years with available meteorological data at the station.

Subscript i represents different station codes. The frequency of different drought levels can be calculated based on the number of years with different drought severities.

2.2.3 Rotated Empirical Orthogonal Function

The REOF (Rotated Empirical Orthogonal Function) analysis method is used for drought regionalization. It is an extension of the traditional Empirical Orthogonal Function (EOF) analysis that incorporates a rotation transformation. The purpose of REOF analysis is to concentrate the high-value areas that are spatially related to the principal components within a smaller range, facilitating the identification of spatial patterns. After rotation, each spatial point is highly correlated with only one principal component. The rotated eigenvector field is more temporally stable compared to the original one. The resulting spatial analysis structure after rotation is clearer, not only reflecting variations in different regions but also indicating the distribution of correlations among different regions. The obtained modes are the rotated factor loading vectors.

2.2.4 Mann-Kendall (MK) test method

When the Mann-Kendall test is used to detect abrupt changes in a series, it involves constructing a rank series.

$$S_k = \sum_{i=1}^k \sum_{j=i+1}^n \alpha_{ij} \quad (k = 2, 3, 4, \dots, n) \quad (14)$$

In which, when $X_i > X_j$, $\alpha_{ij} = 1$; when $X_i < X_j$, $\alpha_{ij} = 0$; where, $j = 1, 2, 3, \dots, n$.

Statistical variables were defined as follows:

$$UF_k = \frac{[S_k - E(S_k)]}{\sqrt{Var(S_k)}} \quad (k = 1, 2, 3, \dots, n) \quad (15)$$

Where,

$$E(S_k) = k(k+1)/4; Var(S_k) = k(k-1)(2k+5)/72$$

Given a significance level (α) and assuming

UF_k follows a standard normal distribution, if

$|UF_k| > U_{\alpha/2}$, it shows that the series has undergone a notable trend change. To further analyze the time series X, it can be rearranged in reverse order, and the calculations according to the aforementioned equation can

be performed while ensuring $UB_k = -UF_k$, $k = n+1-k$.

Analyzing the statistical series UF_k and

UB_k allows for a further examination of the trend changes in the sequence X, including identifying the specific time of the sudden change and indicating the region of abrupt change. The sequence appears to be trending

upward if UF_k is greater than 0; A decreasing trend is indicated if it is less than 0. When these values surpass the critical value, it represents a notable rising or falling trend. In

the event that the UF_k and UB_k curves intersect within the range of the critical threshold, the matching moment of intersection represents the onset of the abrupt change.

3. Results and Analysis

3.1 Spatial Variation of Drought at Annual and Seasonal Scales

3.1.1 Spatial distribution of annual DF

A study on the FDO across the entire province of Jilin was carried out based on the examination of the temporal and spatial features of the SPEI drought index. The frequency values of drought events at an

annual scale ranged from 22% to 40%. On an annual scale, the pattern of drought events' frequency (mean) at various levels was as follows: The order of drought intensity is mild, moderate, severe, and extreme.

The annual DF (Figure 2-A) exhibited a general DT from the southern (Tonghua, Huinan, Huadian) and central-southern (Dehui, Jiutai) regions towards the northwestern part (Qian'an). Additionally, there was a gradual decrease from the southeastern (Luozigou) to the southwestern regions (Antu). The highest DF was observed in Luozigou, Huadian, Dehui, Jiutai, and Nongan regions, followed by Wangqing, Yanji, Tonghua, Liuhe, Huinan, Dongfeng, Erdao, Jiaohe, Shulan, Yushu, Changchun, and Gongzhuling regions, with frequencies exceeding 32%. The frequency of mild drought (Figure 2-a) fluctuated between 3% and 23%, generally decreasing from the southern to the northwestern regions and then gradually from the southeastern to the southwestern regions. The highest frequency was observed in Tonghua, Huadian, and Jingyu regions, exceeding 20%. It was followed by other regions in Tonghua, southern Jilin, Liaoyuan, and eastern Yanbian areas. The frequency of moderate drought (Figure 2-b) fluctuated between 3% and 19%, with an average frequency ranging from 9% to 13%. Overall, it decreased from the northern regions towards the northwestern and southern regions, as well as from the eastern to the southwestern regions. The highest frequencies were observed in Luozigou and Dehui regions, exceeding 17%. It was followed by regions such as Helong, Yushu, Shulan, Nongan, Jiutai, and Taonan, with frequencies above 11%. The frequency of severe drought (Figure 2-c) fluctuated between 0% and 10%, showing a general DT from the northwestern to the southeastern regions. With frequencies above 8%, the regions of Da'an, Changling, Gongzhuling, and Dongfeng showed the highest frequencies. The frequency of extreme drought (Figure 2-d) ranged from 0% to 3.5%. The occurrence of extreme drought was less frequent, with a higher probability in the southeastern regions compared to the northwestern regions. The highest frequencies were observed in Changchun, Shuangyang, Yantongshan, Jingyu, Erdao, Yanji, Longjing, and Ji'an regions. In general, there was consistency between the regularity of

moderate drought occurrences and the overall annual DF. Regions with higher frequencies of mild drought experienced lower frequencies of moderate, severe, and extreme drought. Similar conclusions could be drawn for regions experiencing other levels of drought occurrences.

3.1.2 Spatial distribution of seasonal DF

The frequency of spring drought (Figure 3-a) fluctuated between 26% and 42%, with most areas experiencing frequencies ranging from 26% to 32%. Spring drought was predominantly observed in the southern regions (Liuhe, Tonghua, Jingyu), eastern regions (Dunhua, Antu, Yanji, Erdao, Hunchun, Luozigou, etc.), and northern regions (Tongyu, Yushu). The highest frequency was recorded in Liuhe, reaching over 40%. It was followed by Jingyu, Antu, Yanji, and Tongyu, where frequencies reached around 30%. Overall, the southeastern parts of the region exhibited higher spring drought frequencies compared to the northwest. The frequency of summer drought (Figure 3-b) fluctuated between 27% and 37%. Most areas in the province experienced frequencies above 30%. The highest frequencies were observed in Liuhe, Donggang, Huinan, Panshi, Shuangyang, Gongzhuling, Dehui, Yushu, and Luozigou, with frequencies exceeding 35%. Generally, the central and southern regions exhibited higher frequencies compared to other areas. The frequency of autumn drought (Figure 3-c) fluctuated between 24% and 42%. The frequencies decreased from the central-western regions towards other areas. The northwestern region, particularly Baicheng, also exhibited relatively high frequencies. The highest frequency was recorded in Shuangyang, reaching 40%, followed by Baicheng and Siping, where frequencies reached 38%. The frequency of winter drought (Figure 3-d) fluctuated between 22% and 41%. Overall, the frequencies decreased from the central and western regions towards the northwest and southeast. The highest frequency was observed in Changling, reaching 40%. It was followed by Tongyu, Shuangliao, Jiutai, Shulan, Yitong, and Panshi, where frequencies reached 35%. At a seasonal scale, all four seasons exhibited relatively high frequencies of drought occurrence, with summer, autumn, and winter experiencing higher frequencies than spring.

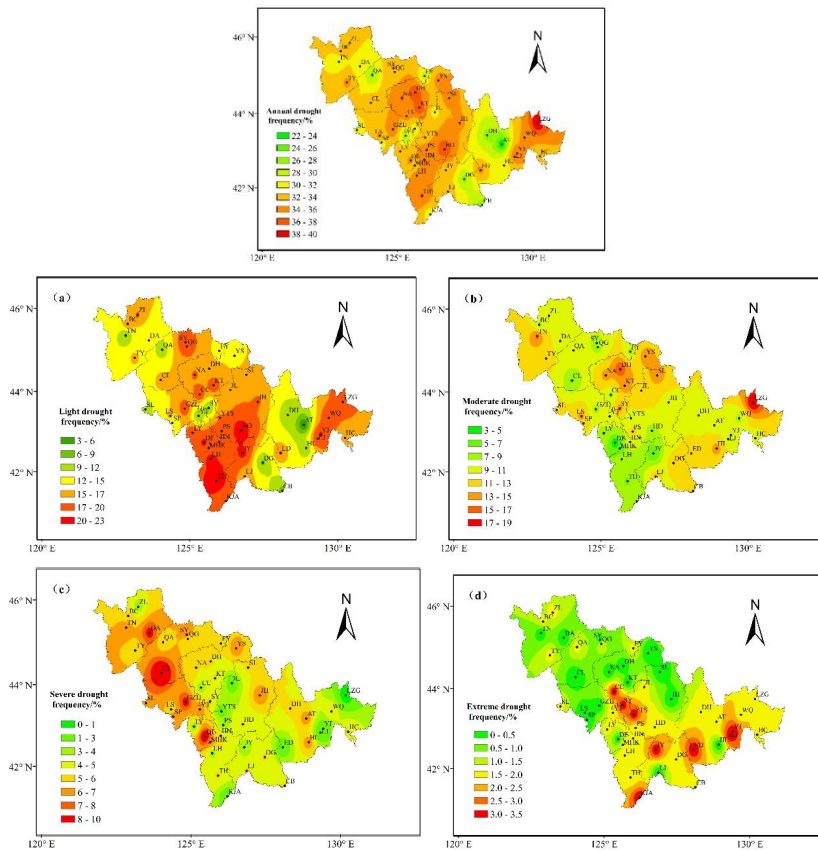


Figure 2. The Spatial Distribution of Annual (Figure 2-A) and (a) Mild, (b) Moderate, (c) Severe, and (d) Extreme Drought Frequencies in the Jilin Region

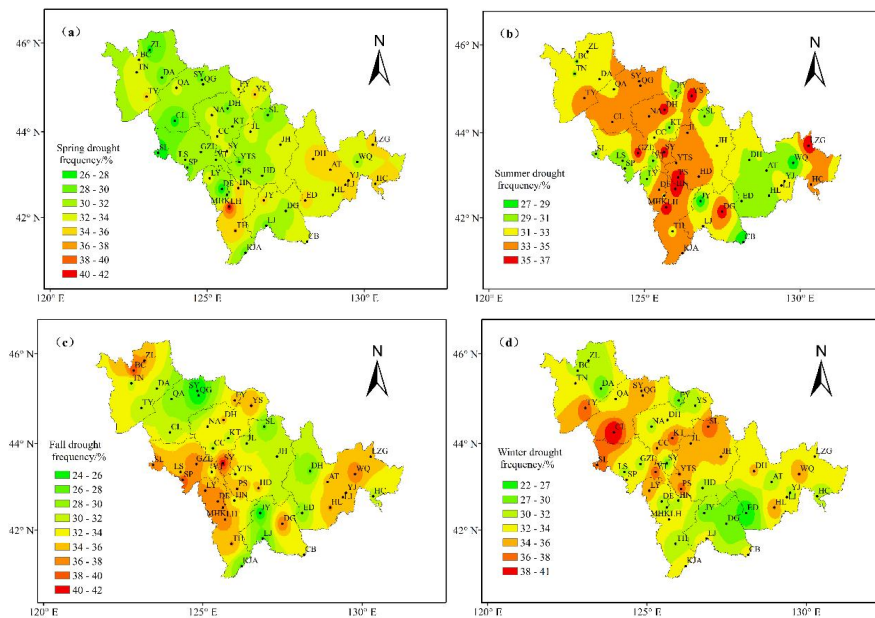


Figure 3. The Spatial Distribution of DF in the Jilin Region for (a) Spring, (b) Summer, (c) Autumn, and (d) Winter Based on SPEI

3.2 Interannual Variation of Drought at the Annual and Seasonal Scale

The average SPEI in Jilin region was mostly positive before 1991, and mostly negative

thereafter, showing significant fluctuations and an overall DT, with a rate of -0.0072 per year (Figure 4-a2). This indicates a tendency towards drought in Jilin region. The annual

SPEI was mostly positive before 1991, but the trend has been continuously decreasing since 1991. After 2004, the DT of SPEI exceeded the critical value of 0.05, indicating a distinct change. The significant turning point of the annual SPEI trend was in 1991, as shown by the point where the UF and UB lines intersect. The spring SPEI showed the smallest trend among the four seasons, with an overall IT and a rate of 0.0043 per year, indicating the most stable spring drought conditions in Jilin region (Figure 4-b2). Furthermore, the MK test results for spring SPEI showed no significant trend, as indicated by the UF and UB lines consistently staying near zero. The increasing and decreasing trends did not exceed the critical value of 0.05.

The DT of summer SPEI was higher than the DT of annual SPEI, with a rate of -0.0085 per year (Figure 4-c2). The trend of summer SPEI changes was consistent with the overall trend of annual changes. The MK test results for summer SPEI indicated a DT before 1982, an IT from 1982 to 1995, and a DT after 1995. The intersection of UF and UB lines occurred multiple times between 1970 and 1995, indicating a signal of IT during 1982-1995, and a DT in summer SPEI after 1995, suggesting a drought tendency in Jilin region during summer after 1995.

The DT of autumn SPEI was higher than the DT of annual SPEI, with a rate of -0.0099 per year (Figure 4-d2). The general tendency of SPEI was decreasing. The MK test results for autumn SPEI indicated a DT before 1967, an IT from 1967 to 1994, and a DT after 1994. The intersection of UF and UB lines indicated a trend change in autumn SPEI in 1967 and 1994. After 2005, the DT exceeded the critical value of 0.05, indicating a significant trend towards autumn drought.

Winter showed the most prominent trend among the four seasons, with a rate of 0.0157 per year (Figure 4-e2). The general tendency of SPEI was increasing during winter, suggesting a tendency towards moist conditions. The UF and UB lines intersected in 2005 and 2009, with an IT after 2009, indicating a trend change in 2009.

3.3 Analysis of the Characteristics of the Main Modes of Drought in Jilin Region

3.3.1 Delineation of drought areas

According to the North criterion, regions with absolute load values greater than or equal to 0.14 and connected as a whole in the same rotated load vector field are classified as the same area. For overlapping areas, they are reclassified based on administrative boundaries[10]. Finally, the drought index in Jilin region is divided into four regions (Figure 5), named as Eastern Zone IV, Southern Zone III, Central Zone II and Northwest Zone I. Zone I includes the northwest part of Jilin, corresponding to 16 representative stations; Zone II includes the central part of Jilin, corresponding to 12 representative stations; Zone III includes the southern part of Jilin, corresponding to 9 representative stations; and Zone IV includes the eastern part of Jilin, corresponding to 10 representative stations.

3.3.2 Spatial distribution of rotated load vector field

REOF analysis was conducted on the average annual SPEI data from 1961 to 2018 in Jilin region. The cumulative variance contribution of the first four eigenvalues accounted for 71.98%. The contribution rate of the first eigenvalue was the highest at 29.81%, followed by 18.29% for the second eigenvalue, 12.61% for the third eigenvalue, and 11.27% for the fourth eigenvalue. The corresponding spatial distribution of the load vector field and time coefficients can be seen in Figure 6.

For the first mode, the load values showed a decreasing pattern from northwest to southeast, with high values in the western part of Jilin, and the maximum value (0.30) was in the central region (Baicheng area) [Figure 6-a]. The time coefficients of this mode showed two distinct periods of change. Before 1992, the coefficients were mostly positive, indicating a relatively low FDO. However, after 1992, there was a significant reversal of wetness and dryness in the northwest region, leading to an IT of drought.

The second mode had a variance contribution rate of 18.29%. The high load values were concentrated in the central part of Jilin, with the maximum value (0.28) in the central region (Jilin area) [Figure 6-b]. The time coefficients of this mode did not show a clear trend and exhibited an alternating pattern in the occurrence of drought years.

The third mode had a variance contribution rate of 12.61%. The load values showed a spatial distribution with greater values in the

southeast and inferior values in the northwest, with the maximum value (0.36) in the central region (Yanbian area) [Figure 6-c]. The time coefficients of this mode exhibited intermittent changes, with a transition from wetness in the 1960s to a significant reversal of wetness and dryness in the 1970s. After the 1990s, the region transitioned from wetness to increasing drought intensity. The fourth mode had a variance contribution

rate of 11.27%. The distribution of load values revealed that the maximum value (0.40) was located in the middle region, with greater values in the southern and western sections and lower values in the northern half (southern areas of Tonghua and Baishan) [Figure 6-d]. The time coefficients of this mode did not show a clear trend, but after 1997, drought events became more frequent, which caused the southern region's drought to get worse

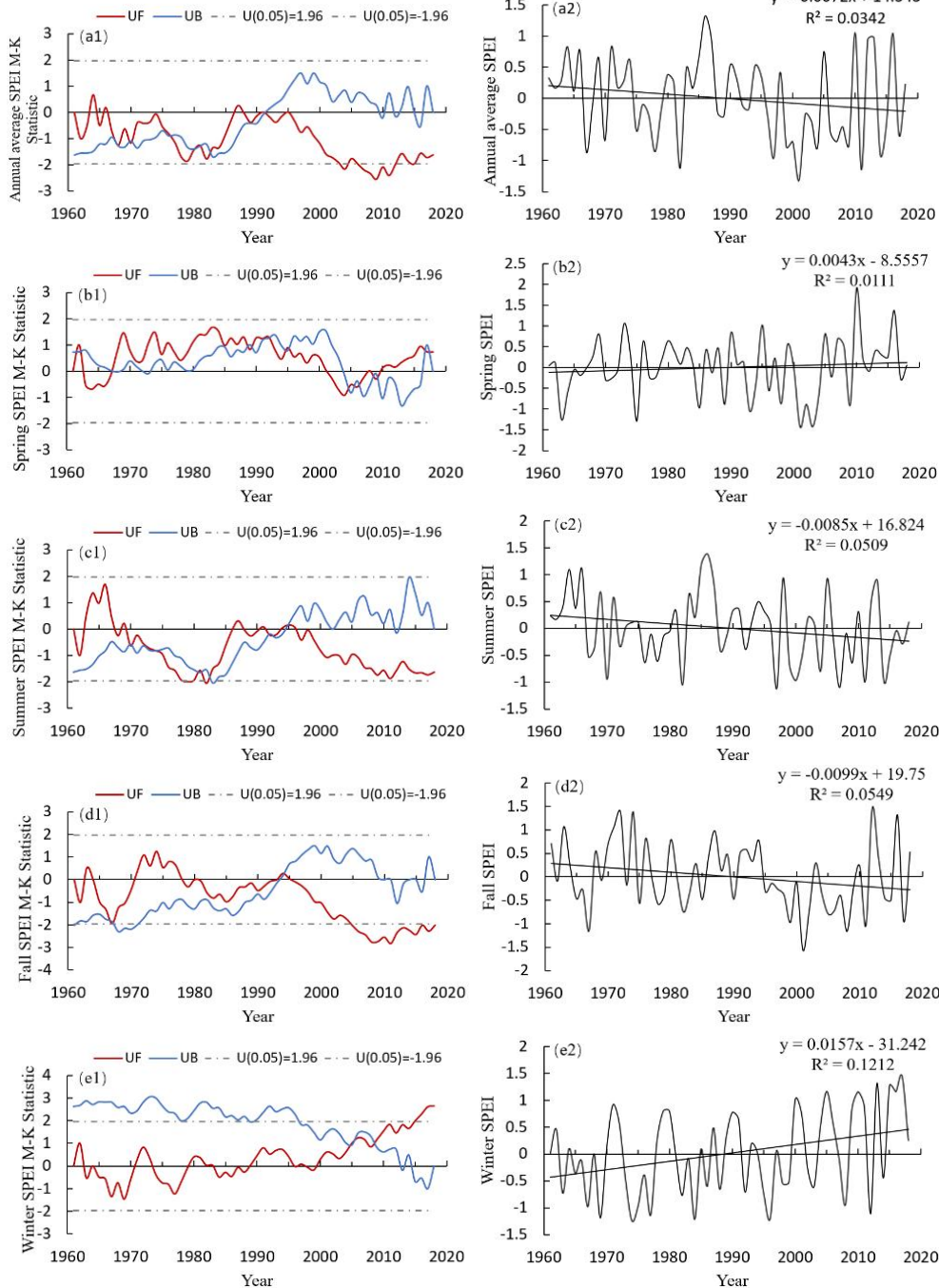


Figure 4. The M-K Test Curve and Interannual Variation Trends in the Jilin Region for (a) Annual, (b) Spring, (c) Summer, (d) Autumn, and (e) Winter Based on SPEI

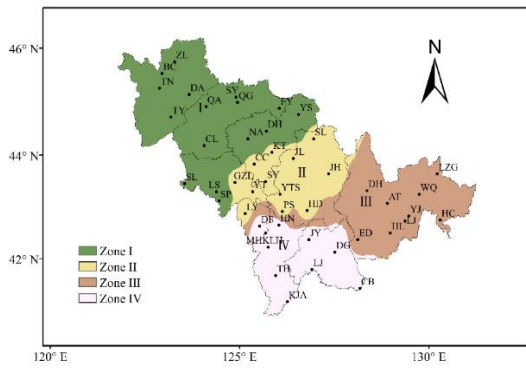
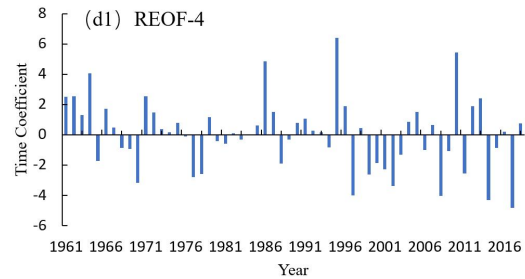
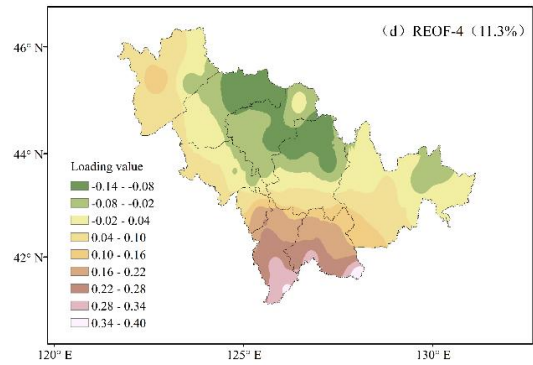
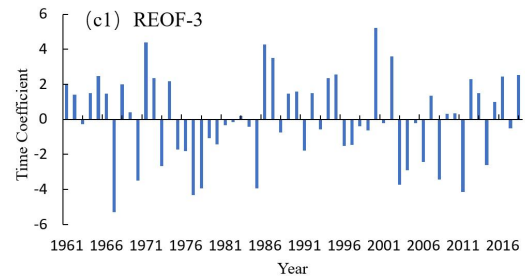
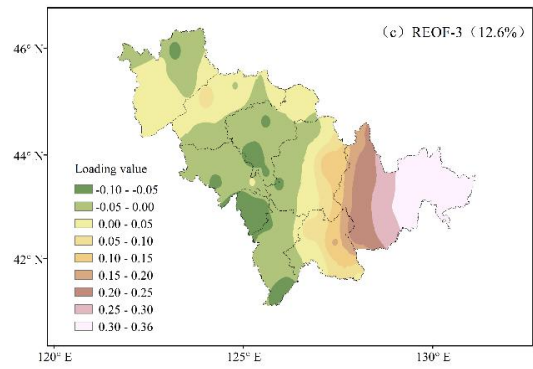
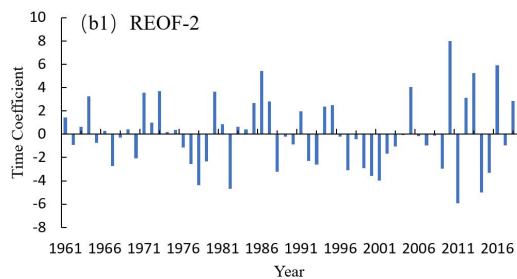
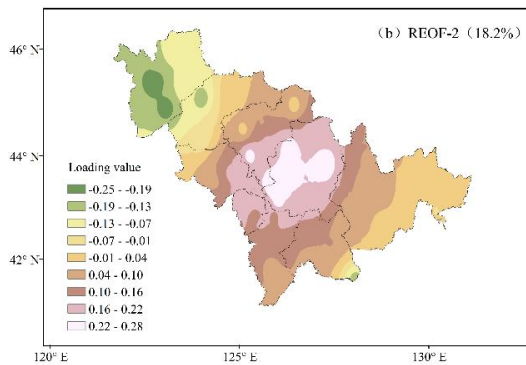
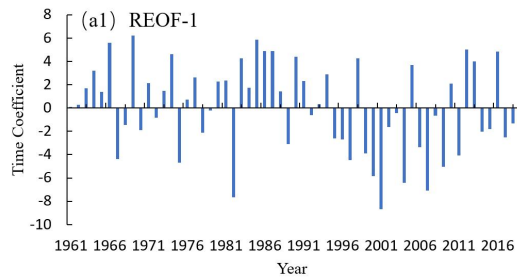
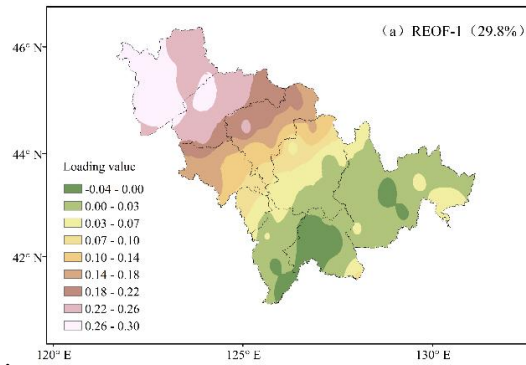


Figure 5. Drought Zoning in Jilin Region



Note a, b, c, and d refer to the first, second, third, and fourth characteristic vectors, respectively. a1, b1, c1, and d1 refer to the time coefficients of the first, second, third, and fourth modes, respectively.

Figure 6. REOF Decomposition Results and Time Coefficients of Drought Characteristic Vectors for SPEI in Jilin Region.

4. Conclusion

This study used the Thornthwaite method in conjunction with monthly temperature and precipitation data from 47 meteorological stations in the Jilin region from 1961 to 2018

to calculate annual and seasonal SPEI. The drought occurrence frequency was analyzed for the entire year, each season, and different drought levels. For the previous 58 years in Jilin, the patterns of drought evolution at the annual and seasonal levels were investigated using the Mann-Kendall test and REOF. The outcomes showed the following conclusions:

1. The annual DF in Jilin region ranged from 22% to 40%. The frequency of droughts on average was (in order of severity) mild, moderate, severe, and extreme. The regions with high frequencies of mild drought also had relatively low frequencies of moderate, severe, and extreme drought. Similar conclusions were observed for different drought levels. At the seasonal scale, the FDO was relatively high for all four seasons, with higher frequencies in summer, autumn, and winter compared to spring.

2. The average annual SPEI in Jilin region was mostly positive before 1991 but became predominantly negative afterwards. It exhibited significant fluctuations and indicated an overall DT, with a trend rate of -0.0072 per year, indicating a general tendency towards increased aridity in Jilin. The year 1991 marked a significant shift towards aridity. Among the four seasons, the change in spring SPEI had the smallest trend, showing an overall IT. The trend in summer SPEI was consistent with the annual trend. The DT in autumn SPEI was the highest among all seasons, and the trend towards aridity became more significant after 2005. The trend rate for winter SPEI was 0.0157 per year, suggesting the most pronounced trend among all seasons, with a tendency towards increased moisture.

3. The REOF analysis allowed for the classification of Jilin region into four drought characteristic zones: northwest, central, south, and east. After 1992, the northwest region experienced a significant reversal between wet and dry conditions, with an IT towards aridity. The central region showed no apparent trend in its time coefficients. The time coefficients for the east region exhibited intermittent changes, with a wetter period in the 1960s, a noticeable reversal between wet and dry conditions in the 1970s, a transition from wetness to aridity after the 1990s, and an intensification of aridity after 2001. The time coefficients for the south region showed no clear trend, but the FDO increased after 1997,

indicating a worsening trend of aridity.

References

- [1] Svoboda M, LeCompte D, Hayes M, et al. The drought monitor. *Bulletin of the American Meteorological Society*, 2002, 83(8): 1181-1190.
- [2] Zamanian M.T, Behyar M. B, Karimi H. A, et al. Agricultural drought monitoring and analysis using remotely sensed data from NOAA-AVHRR. *Journal of Climate Research*. 2012.3(9):102-103.
- [3] Xin X, Yu R, Zhou T, et al. Drought in late spring of South China in recent decades. *Journal of Climate*, 2006, 19(13):3197-3206.
- [4] Zhu Shanshan. Study on drought distribution pattern and trend prediction in western Jilin Province. Northeast Normal University, 2012.
- [5] Vicente-serrano S M, Beguería S, López Moreno JI. A Multiscalar Drought Index Sensitive to Global Warming: The Standardized Precipitation Evapotranspiration Index. *Journal of Climate*, 2010, 23(7):1696-1718.
- [6] Xu Yidan, Ren Chuanyou, Ma Xida, et al. Comparative analysis of multi-time scale drought variation characteristics in Northeast China based on SPI/SPEI index, *Arid Zone Research*, 2017, 34(6): 1250-1262.
- [7] Li Weiguang, Yi Xue, Hou Meiting, et al. Standardized precipitation evapotranspiration index shows drought trends in China. *Chinese Journal of Eco-Agriculture*, 2012, 20(5): 643-649.
- [8] Wang Lin & Chen Wen. Applicability Analysis of Standardized Precipitation Evapotranspiration Index in Drought Monitoring in China. *Plateau Meteorology*. 2014, 33(2): 423-431
- [9] Ma J Z & Hao L. Temporal and spatial variation of drought in the Xilingol grassland based on the standardized precipitation index and standardized precipitation evapotranspiration index. *Pratacultural Science*, 2021, 38(12): 2327-2339.
- [10] Yang Chengfang. Analysis of REOF on body comfort in Shandong. *Journal of the Meteorological Sciences*, 2006, (1):103-109